

Chapter IV

Results and discussion

This research focused on the effects of operational parameters on the photocatalytic-reduction efficiency of chromium (VI) with TiO₂ thin films fixed bed photoreactor in order to find the optimum operational parameters. Effects of each operational parameter on treatment ability of fixed bed photo-reactor were measured in terms of residual fraction of chromium (VI) concentration solution in term of C/C_0 . The studied parameters included initial pH of wastewaters, feed flow rate, water level of wastewaters, active surface area and initial concentration. This research was divided into 6 parts as follows:

Experiment 1 – thin film characteristic

Experiment 2 – effect of pH

Experiment 3 – effect of flow rate

Experiment 4 – effect of water level of waste water

Experiment 5 – effect of active surface of catalyst

Experiment 6 – effect of initial concentration

4.1 Reactor designing

4.1.1 Fixed bed photocatalytic reactor (FBPR) design

The reactor configuration was planned to be a rectangular aluminum box with two hyperbolic roofs for light concentration with UV lamps within reactor. Aluminum was appropriate for produced the body of this reactor as it provide high reflection of light to the system. This reactor has 5 baffles including six sections. Two UV lamps (Philips TLK/05 40 Watt, 380 nm.) set on each arc roof. This reactor was designed for

continuous flow which be controlled by pump (LIFE TECH-AT1600, 900 liter/hours, 1.1 Hmax, AC200/240 Volt, 50 Hz and 51/60 Watt) and valves for control water level and feed flow rate.

Each section of FBPR set 3 TiO_2 thin film plates. All over sections have 18 plates that show in Figure 4.2. The Figure 4.1 shows photograph of FBPR and Figure 4.2 illustrates the model of FBPR. Summary of the dimensions of the FBPR shows in Table 4.1.

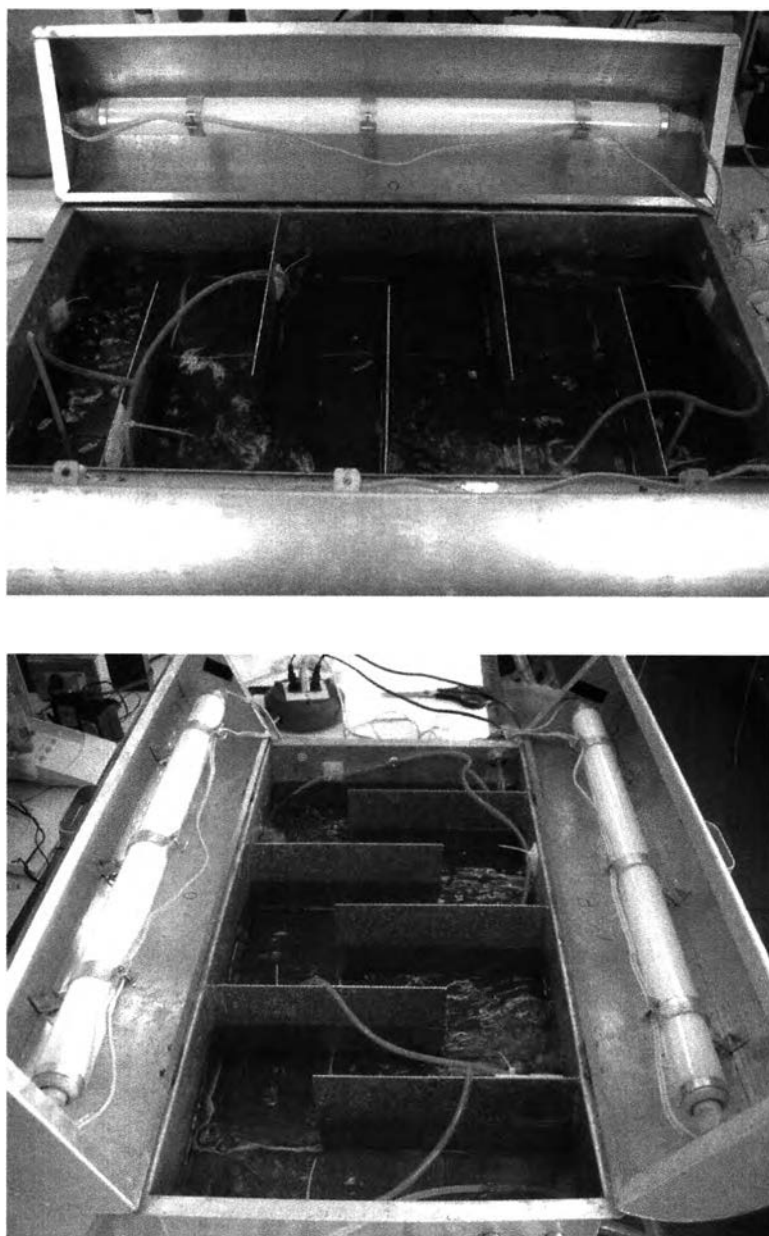
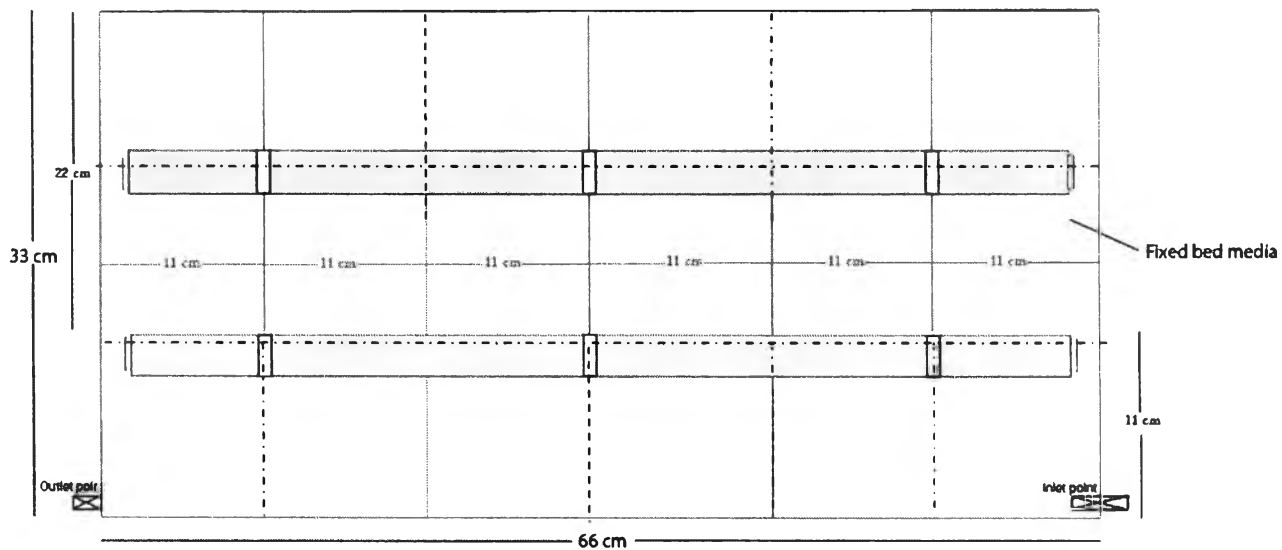
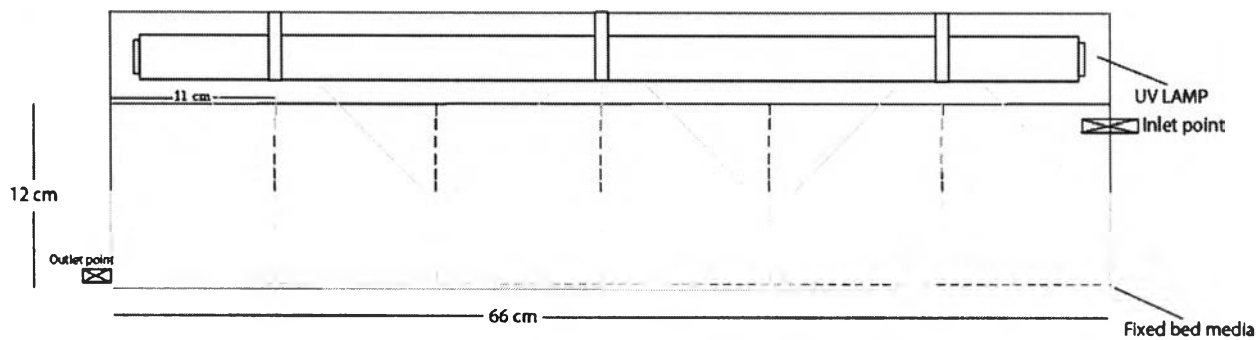


Figure 4.1 Photograph of fixed bed photocatalytic reactor

• **Top View**



• **Front View**



• **Side View**

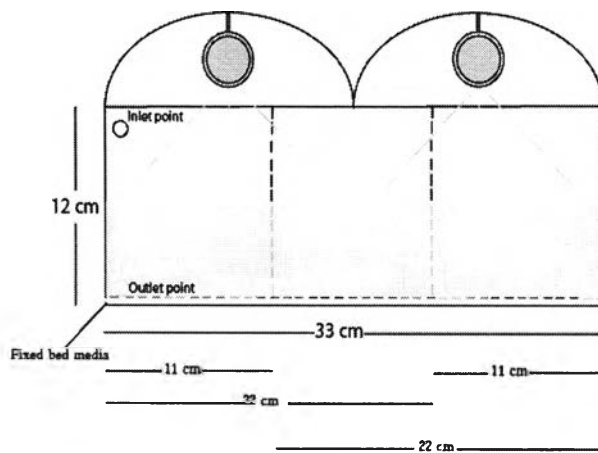


Figure 4.2 The dimensions of fixed bed photocatalytic reactor

Table 4.1 Dimensions of fixed bed photocatalytic reactor

Length of reactor (cm.)	66.00
Width of reactor (cm.)	33.00
Height of reactor (cm.)	12.00
Length of plates (cm.)	10.80
Width of plates (cm.)	10.60
Number of plates	18
Total thin film area per 1 plate (cm ²)	114.48
Total thin film area of plates (cm ²)	2060.64

4.1.2 Performance of the Fixed bed photocatalytic reactor

In this reactor, wastewater was fed into a reactor and passed through a media that was coated by catalyst while mixing of the wastewater is a by turbulent flow of wastewater stream and gas purging. Mixing and adsorption process provided high levels of available attached TiO₂. When irradiation of UV lamp goes through reactor, the photocatalysis process occurs. The contaminants reacted with catalyst and attach to surface of the media.

4.2 Experiment 1-thin film characteristic

4.2.1 Thin film characteristic morphology analysis by scanning electron microscope (SEM)

Figure 4.3 shows the SEM micrograph of the stainless steel surface without TiO₂. This figure shows stainless grain and surface. Figure 4.4 shows the SEM micrograph of the 3 cycled coated TiO₂ thin films stainless steel surface. The figure shows that at 3 cycles, smooth surface and low fracture were observed.

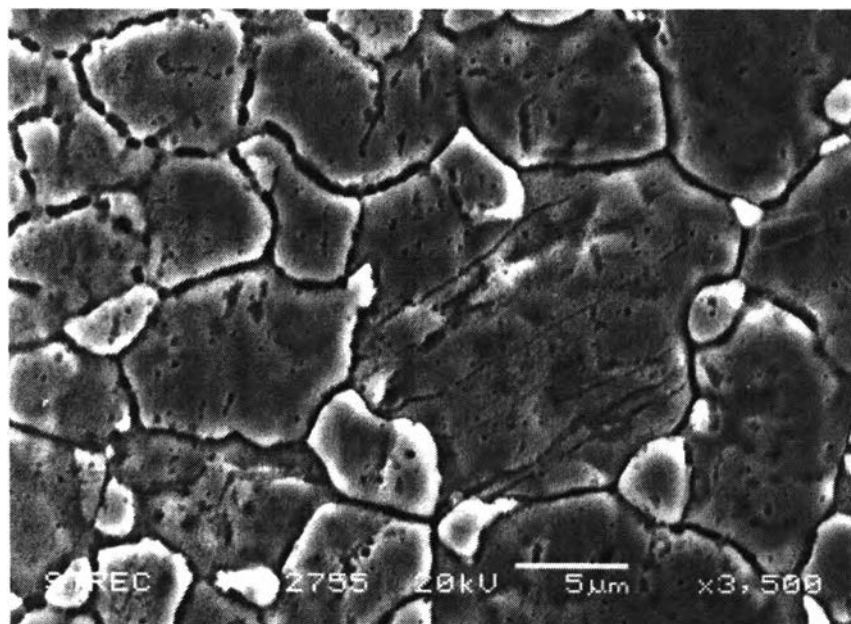


Figure 4.3 SEM micrograph of the stainless steel surfaces without TiO₂ at 3,500 x magnifications

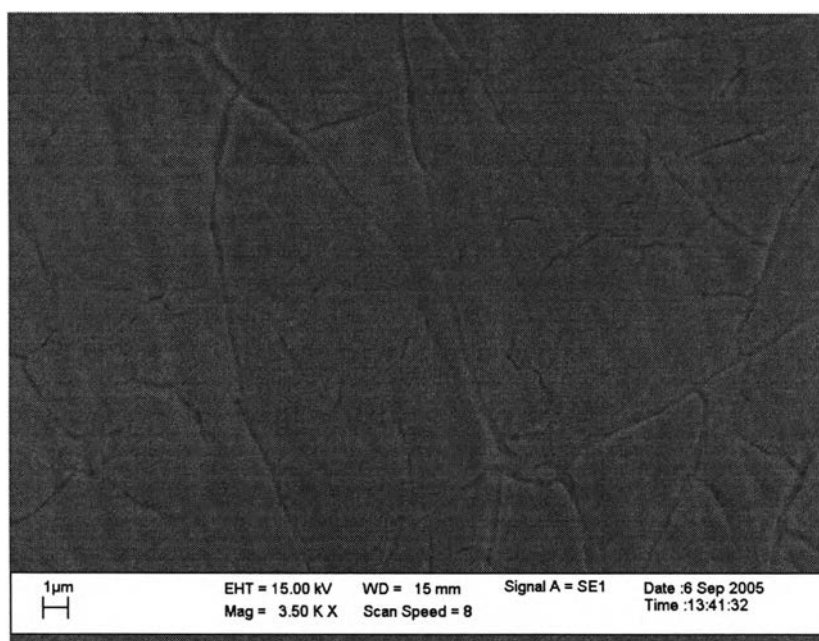


Figure 4.4 SEM micrograph of the 3 cycled coated TiO₂ thin films stainless steel surface at 3,500 x magnifications

From the morphology of TiO_2 thin film that observed by FE-SEM as shown in Figure 4.5, the thickness of 3 cycled coated TiO_2 thin film equaled to 91 nm could be investigated.

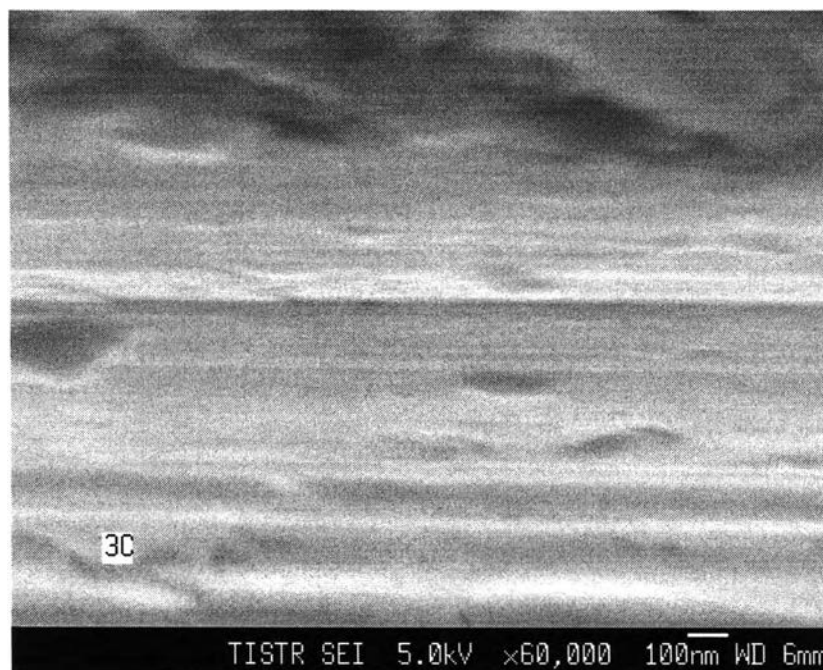


Figure 4.5 Morphology of the 3 cycled coated TiO_2 thin films

4.2.2 Formation structure analysis by X-Ray Diffraction (XRD)

The formation structure was observed by X-Ray Diffraction (XRD) analysis. Figure 4.6 show the XRD pattern of the 3 cycled coated TiO_2 thin films on the stainless steel surface. From this figure, it can be observed high amount of anatase type crystal structure form of TiO_2 at 3 cycles and calculate crystallite size can also be observed by line broadening measurements in the Debye-Scherrer equation as shown in Equation (16) chapter 2.

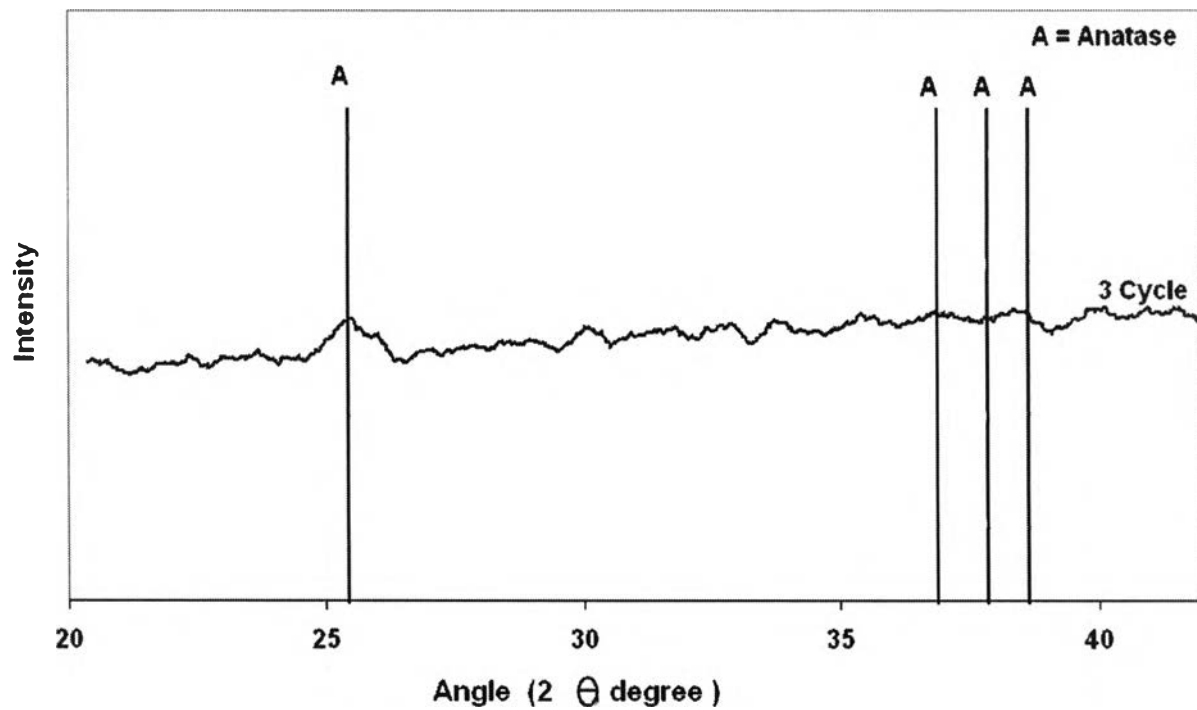


Figure 4.6 XRD patterns of the 3 cycled coated TiO₂ thin films

From Figure 4.6, the crystallite size can be calculated as follow:

$$L = \frac{0.89 \times 0.15418}{0.01396 \times \cos\left(\frac{25.48}{2}\right)} = 10.078 \text{ nm}$$

Mass of 3 cycled coated TiO₂ thin films per 1 plate was obtained by weighing measurement and average that approximately 0.0200 g/plate. Figure 4.7 shows stainless steel plate with and without TiO₂.

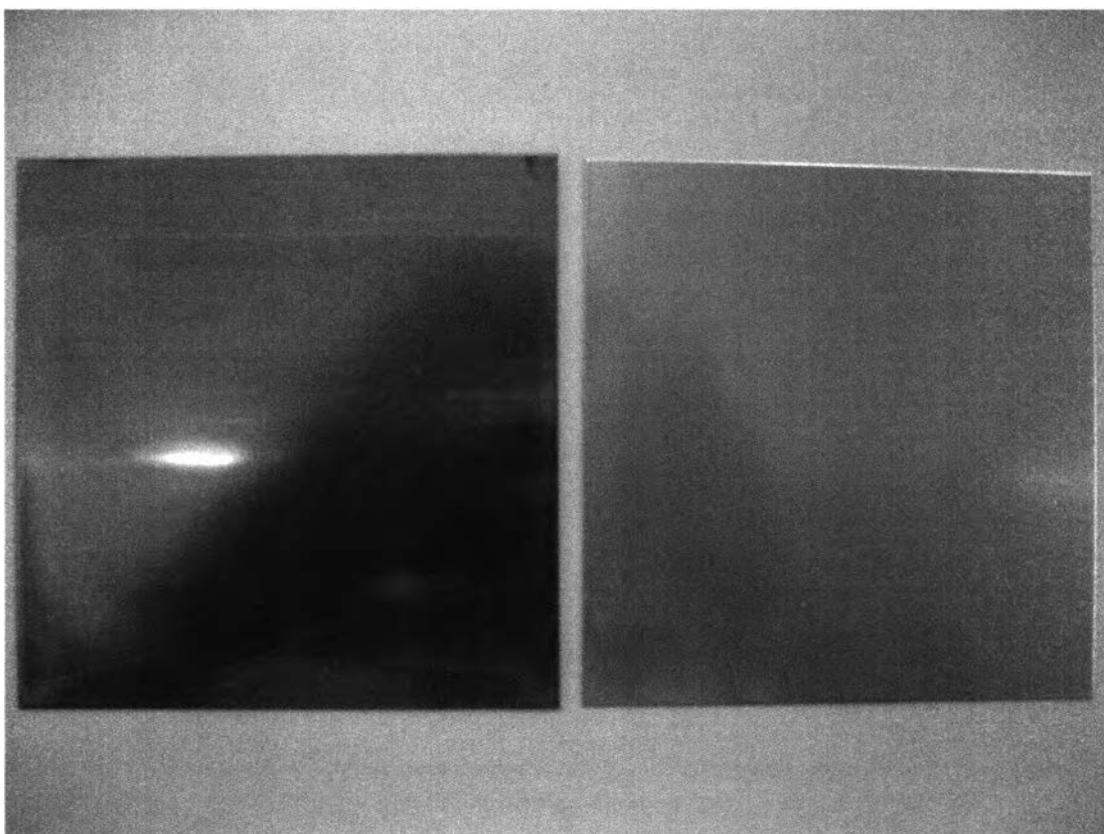


Figure 4.7 Stainless steel plates with and without TiO₂

4.3 Experiment 2 – effect of pH of wastewaters

The pH values of wastewaters in this study were varied as 3, 7, and 11. The pH adjustment was done by sulfuric acid (H₂SO₄) or sodium hydroxide (NaOH).

The fixed parameters in this research were set at 25 ppm of initial chromium (VI) concentration of 20 L synthetic wastewaters. The feed flow rate of wastewaters was 80 mL/sec. The water level in the fixed bed reactor was 4 cm.

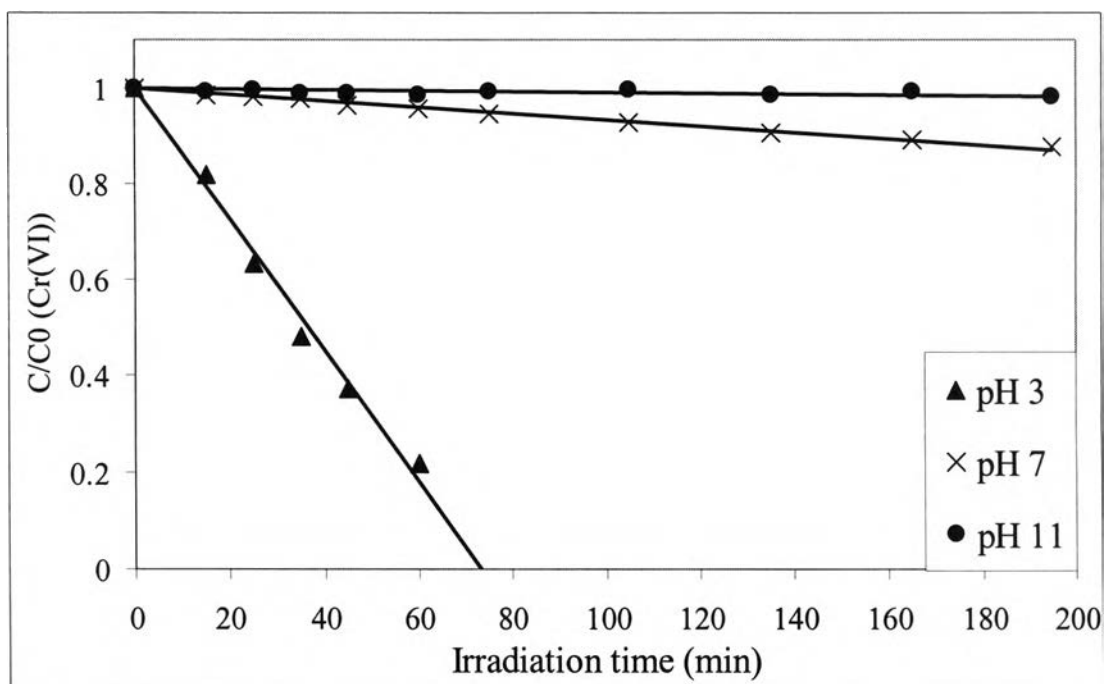


Figure 4.8 Effect of pH of wastewaters on photocatalytic-reduction of chromium (VI) with time ($[\text{Cr (VI)}] = 25 \text{ ppm}$, feed flow rate 80 mL/sec and water level 4 cm.)

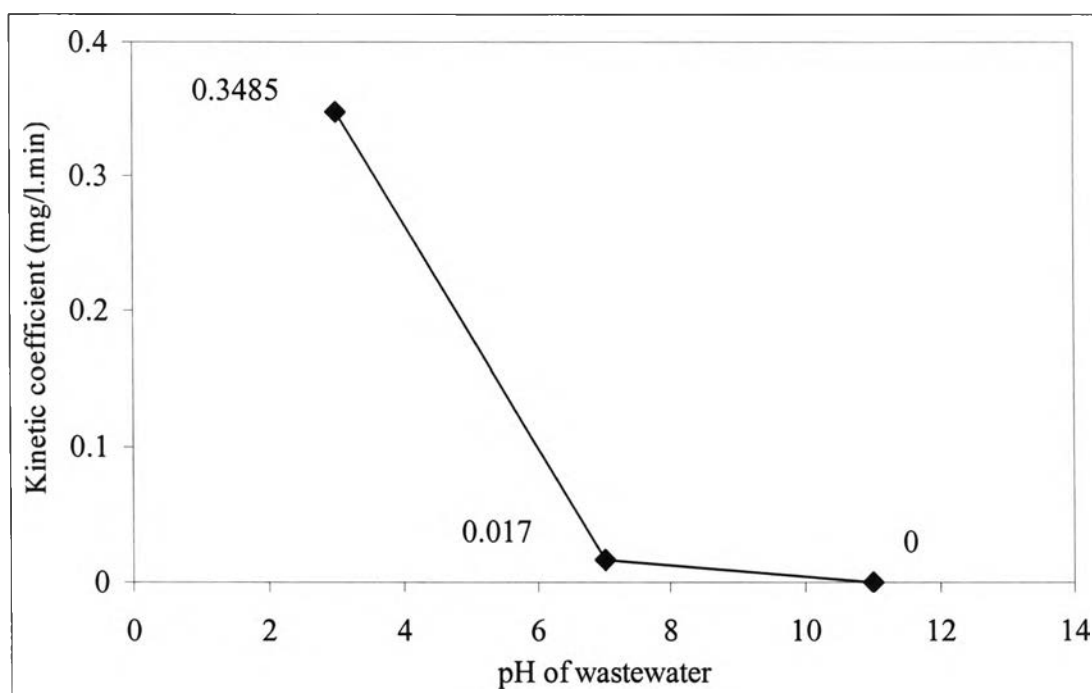


Figure 4.9 Kinetic coefficients (k) of chromium (VI) at different pH

Table 4.2 Experimental conditions and important parameters in variation of pH

Parameter	Experiment		
	3	7	11
pH of wastewaters	3	7	11
Cr (VI) adsorption after 15 min, (mg/L)	4.52	0.36	0
Cr (VI) removal percentage at 74 min of reaction period, (%)	100	5.18	0
Kinetic coefficient (<i>k</i>), mg/L.min)	0.3485	0.017	0

From Figure 4.8, the chromium (VI) degradation was zero order which can be calculated kinetic coefficient (*k*) by zero order equation as shown in Equation (12) chapter 2. Figure 4.9 shows that the highest kinetic coefficient was observe at pH 3 of wastewaters and it was 0.3485 mg/L.min. As pH of wastewater increased, the kinetic coefficient was decreased.

From Figure 4.8, it was found that at pH 7 the efficiency in Cr (VI) removal was decreased. At pH 11, as shown in graph, neither adsorption nor reduction takes place. The reason which might be explained by the fact that at pH above 7, the photocatalyst surface become negative which repels the chromate ion (CrO_4^{2-}). By contrast, at pH 3, chromium (VI) was effectively removed by fixed bed photocatalytic reactor within 74 minute. The explanation came from the surface effect as at low pH the photocatalyst surface become positive and can attract HCrO_4^- ion on the surface.

Besides the adsorption effect, the difference in reduction potential was another reason. At pH3, the difference between the reduction potential of the $\text{Cr}^{+6}/\text{Cr}^{+3}$ and the relative reduction potential of conduction band of TiO_2 was higher than that at pH 7 and pH 11 as shown in Figure 2.7. Thus, the photocatalytic reduction of Cr (VI) in pH 3 is much more favorable than pH 7 and pH 11.

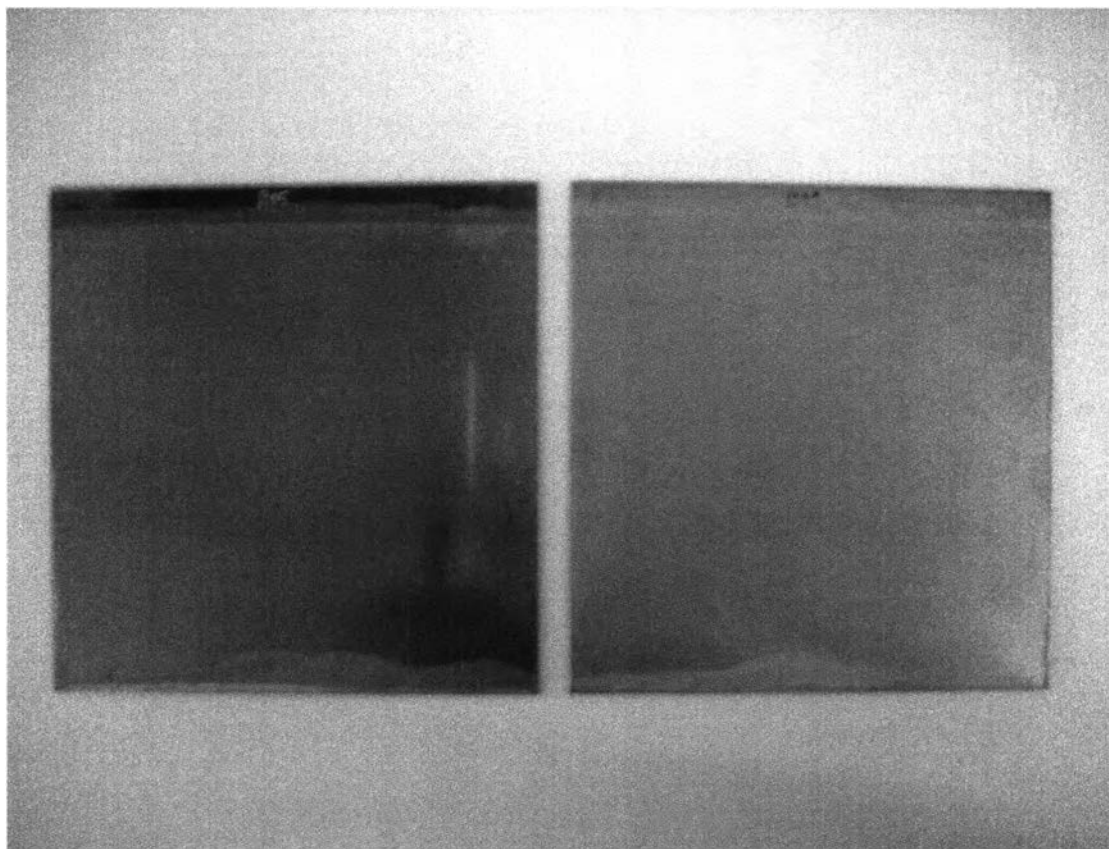


Figure 4.10 TiO_2 thin film plates and used TiO_2 thin film plates

The used TiO_2 thin film plate was colored from golden yellow to white. Figure 4.10 show nonused and used TiO_2 thin film plate.

4.4 Experiment 3 - effect of flow rate of wastewaters

To study the effect of flow rate of wastewaters on photocatalytic reduction of chromium (VI), the flow rate of wastewaters in this study were varied as 20, 40, 60, 80, 100, 120 and 140 mL/sec. The fixed parameters in this research were set at 25 ppm of initial chromium (VI) concentration of 20 L synthetic wastewaters. The water level in the fixed bed reactor was set at 6 cm. The initial pH for photocatalysis reaction was performed at pH 3 obtained from experiment 2.

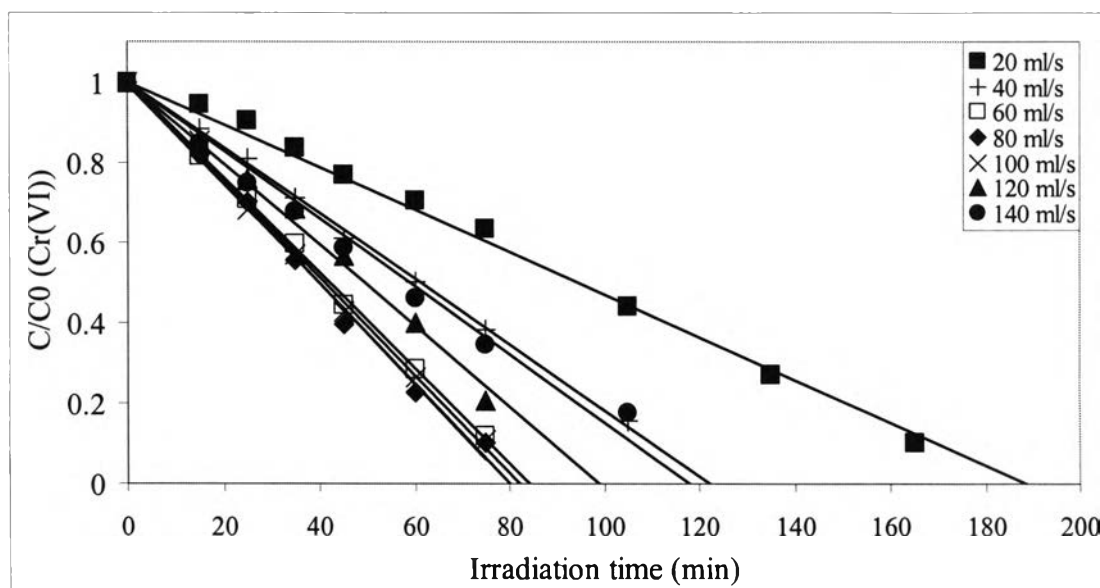


Figure 4.11 Effect of flow rate on the photocatalytic-reduction of chromium (VI) with time ($[\text{Cr (VI)}] = 25 \text{ ppm}$, $\text{pH} = 3$ and water level 6 cm)

From Figure 4.11, it was found that at flow rate of 60, 80 and 100 mL/sec the fixed bed photoreactor could remove chromium (VI) completely rapidly in vicinal time at 84, 80 and 82 minute. As the flow rate of wastewaters was changed to 20, 40, 120 and 140 mL/sec the photoreactor could remove completely chromium (VI) with a longer period at 188, 122, 99 and 118 minute.

From Figure 4.11, the kinetic of chromium (VI) degradation was zero order. The kinetic coefficient can also be calculated by zero order equation as shown in Equation (7) chapter 2. Figure 4.12 shows bell graph shape. When the feed flow rate was increased, the kinetic coefficient increased and it was 0.3129 mg/L.min. Then, when higher flow rate was applied, the kinetic coefficient decreased. From Table 4.3, it was found that contact time related to the treating cycles and treating cycle related to the amount of absorbed chromium (VI). At the lowest flow rate of 20 mL/s, the contact time was 10.89 min/cycle, treating cycles was 7.35 cycle, amount of absorbed chromium (VI) was 1.39 mg/L and chromium (VI) removal efficiency was 42.4 %. At the highest flow rate of 140 mL/s the contact time was 1.56 min/cycle, treating

cycles was 51.42 cycles, amount of absorbed chromium (VI) was 4.85 mg/L and chromium (VI) removal efficiency was 68 %. It shows that the increase in feed flow rate of wastewater provided higher amount of chromium (VI) adsorption which influenced further on amount of chromium (VI) removal in irradiation process.

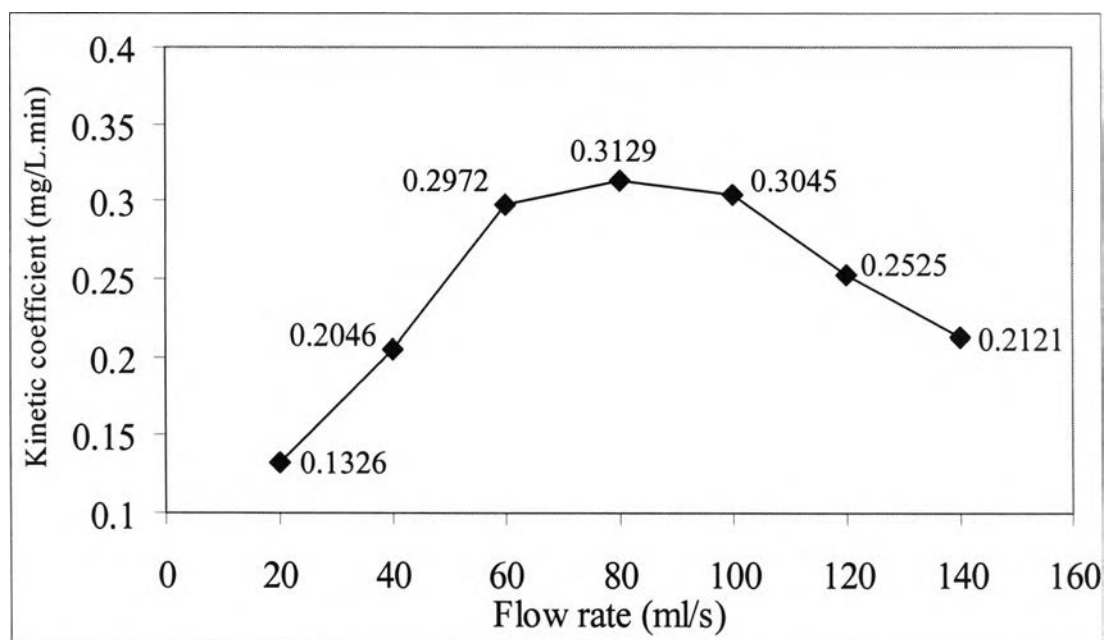


Figure 4.12 Kinetic coefficients (k) of chromium (VI) with different feed flow rate

From Figure 4.12 and Table 4.3, the results could be explained that at low flow rate of wastewaters equaled to 20, 40 and 60 mL/sec, their efficiency were low because these conditions had lowest treating cycles (7.35, 14.69 and 22.04 cycles) that affected on amount of absorbed chromium (VI) decrease (1.39, 2.95 and 4.5 mg/L) and consequently the chromium (VI) removal efficiency. The highest efficiency was observed at middle flow rate equaled to 80 mL/s. This condition had treating cycles equaled to 29.38 cycles and amount of chromium (VI) adsorption equaled to 4.62 mg/L.

Table 4.3 Experimental conditions and calculation of important parameters in variation of flow rates

Parameter	Experiment						
	20	40	60	80	100	120	140
Flow rate, (mL/sec)	20	40	60	80	100	120	140
Water level, (cm)	6	6	6	6	6	6	6
Contact time, (min/cycle) If reaction period is 80 min	10.89	5.45	3.63	2.72	2.18	1.82	1.56
Treating cycle, (cycle) If reaction period is 80 min	7.35	14.69	22.04	29.38	36.73	44.08	51.42
Cr (VI) adsorption after 15 min, (mg/L)	1.39	2.95	4.5	4.62	4.68	4.91	4.85
Cr (VI) removal percentage at 80 min of reaction period, (%)	42.4	65.6	95.2	100	97.6	80.8	68
Kinetic coefficient (<i>k</i>), mg/L.min)	0.1326	0.2046	0.2972	0.3129	0.3045	0.2525	0.2121
R ²	0.9943	0.9907	0.9984	0.9933	0.9957	0.9923	0.9806
Reaction time to complete photoreduction of Cr(VI), (min)	188	122	84	80	82	99	118

When the feed flow rate was increased (higher than 80 mL/s), the photo-reduction efficiency was decreased at high treating cycle (36.73, 44.08 and 51.72 cycles), amount of absorbed chromium (VI) was 4.68, 4.91 and 4.85 mg/L and the efficiency in chromium (VI) removal was 97.6, 80.8 and 68 %. It could be explained that at flow rate higher than 80 mL/s the mass transfer limitations was expected to occur. This effect might lead to the decreasing in photocatalytic reduction efficiency.

4.5 Experiment 3 - effect of water levels of wastewaters

To study the effect of water levels of wastewaters on photocatalytic reduction of chromium (VI), the water levels of wastewaters in this study were varied as 2, 3, 4, 5 and 6 cm. The fixed parameters in this research were set at 25 ppm of initial

chromium (VI) concentration of 20 L synthetic wastewaters. The feed flow rate of wastewaters was set at 80 mL/sec as obtained from experiment 3. The initial pH for photocatalysis reaction was performed as pH 3 as obtained as shown in Equation (12) chapter 2.

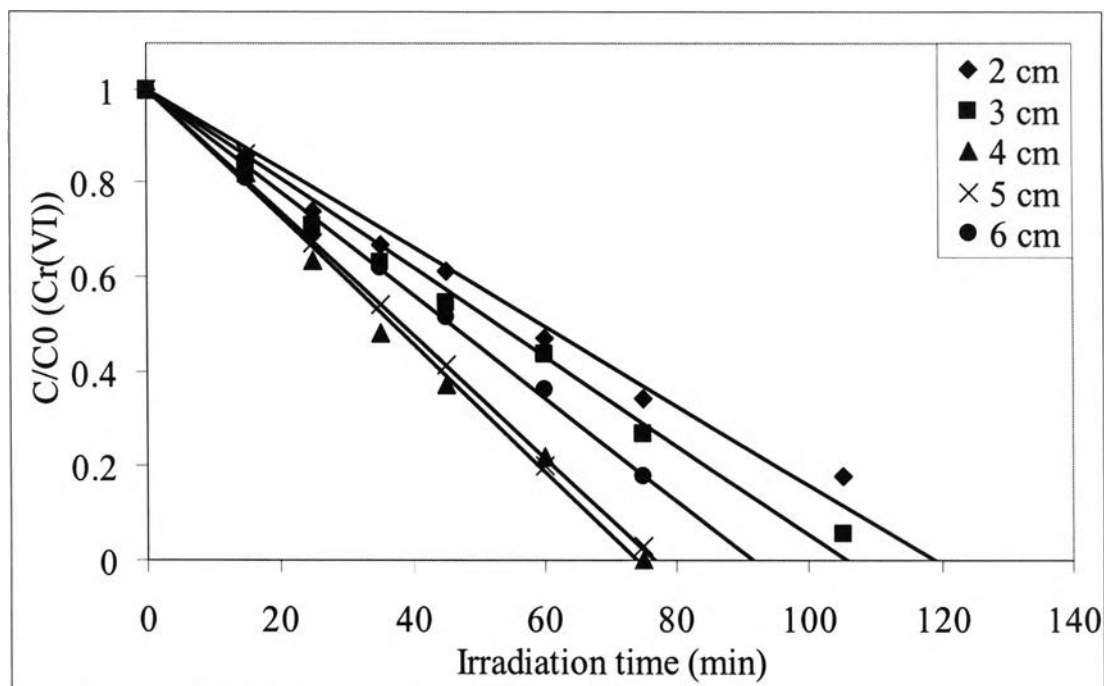


Figure 4.13 Effect of water level on photocatalytic-reduction of chromium (VI) with time ($[\text{Cr (VI)}] = 25 \text{ ppm}$, $\text{pH} = 3$ and flow rate 80 mL/sec)

From Figure 4.13, it was found that at 4 and 5 cm of water level the fixed bed photoreactor could remove chromium (VI) completely in vicinal time at 74 and 78 minute. As the water level of wastewaters was changed to 2, 3 and 6 cm the photoreactor could remove completely chromium (VI) with a longer period at 119, 105 and 92 minutes, respectively.

From Figure 4.13 the kinetic of chromium (VI) degradation was zero order. The kinetic coefficient can also be calculated by zero order equation from Equation (7). Figure 4.16 shows bell graph shape. When the water level was increased, the kinetic coefficient was increased and it was 0.3485 mg/L.min. Then, when higher water level was applied, the kinetic coefficient was decreased. From Table 4.4, it can be found that water level related to the volume of water in reactor and amount of

chromium(VI) adsorption. At the lowest water level of 2 cm, the volume of water in reactor was 4,356 mL, amount of adsorbed chromium (VI) was 3.56 mg/L and chromium (VI) removal efficiency was 62.4 %. At the highest water level of 6 cm the

Table 4.4 Experimental conditions and calculation of important parameters in variation of water level

Parameter	Experiment				
Water level, (cm)	2	3	4	5	6
Flow rate, (mL/s)	80	80	80	80	80
Volume of water in reactor, (mL)	4,356	6,534	8,712	10,896	13,068
Cr (VI) adsorption after 15 min, (mg/L)	3.56	4.08	4.52	4.45	4.76
Cr (VI) removal percentage at 74 min of reaction period, (%)	62.24	69.76	100	96.35	80.28
Kinetic coefficient (k), (mg/L.min)	0.2168	0.2352	0.3485	0.3256	0.2739
R^2	0.9885	0.9867	0.9934	0.9941	0.9946
Reaction time to complete photoreduction of Cr(VI), (min)	119	105	74	78	92

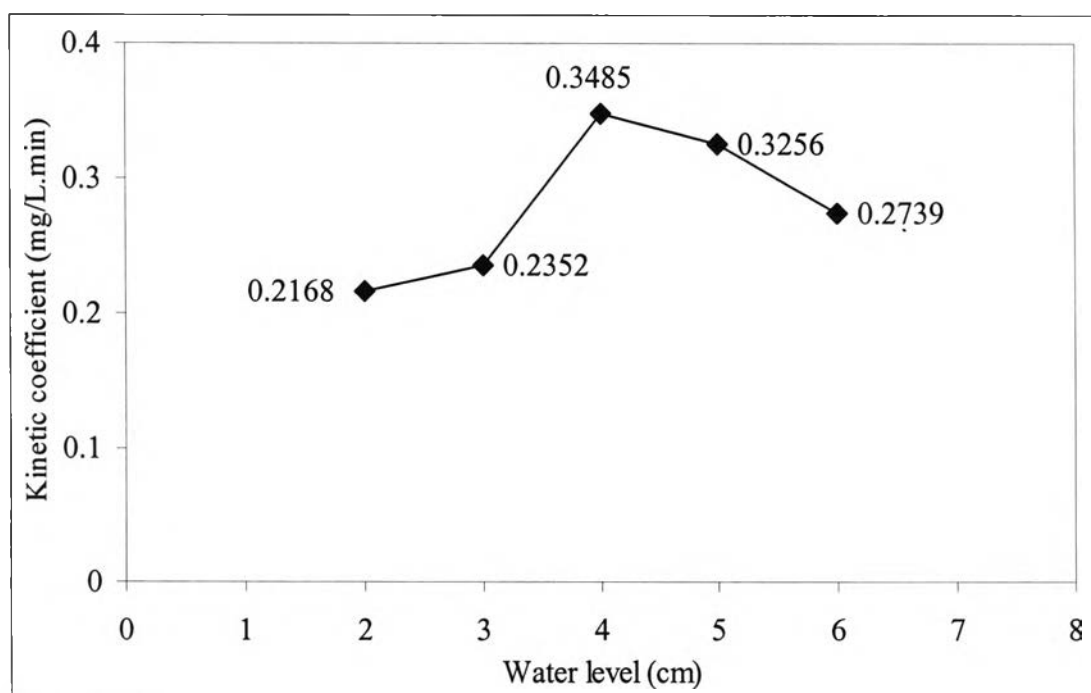


Figure 4.14 Kinetic coefficients (k) of chromium (VI) with different water levels

volume of water in reactor was 13,068 mL, and amount of absorbed chromium (VI) adsorption was 4.76 mg/L and chromium (VI) removal efficiency was 80.28 %. It shows that the increase in water level in reactor provide higher amount of chromium (VI) adsorption, which influence further on amount of chromium (VI) removal in irradiation process.

From Figure 4.14 and Table 4.4 it could be explained that at low water level of wastewaters equaled to 2, and 3 cm, their efficiency was low because these conditions had lowest volume of water in reactor (4,356 and 6,534) that effect to amount of absorbed chromium (VI) decrease (3.56 and 4.08 mg/L) and consequently the chromium (VI) removal efficiency. The highest efficiency was observed at middle water level equaled to 4 cm this condition had volume of water in reactor equaled to 8,712 mL, amount of chromium (VI) adsorption equaled to 4.52 mg/L, and chromium (VI) removal efficiency was 100 %.

When the water level was higher than 4 cm, the photo-reduction efficiency was decreased even though they had high volume of water in reactor (10,896 and 13,068 mL) and amount of chromium (VI) adsorption (4.45 and 4.76 mg/L). It could be explained that at high water level of wastewaters equaled to 5 and 6 cm the thickness of wastewaters might affect by intensity of UV lamp that irradiated to TiO₂ surface. With less intensity of UV light reaching the TiO₂ surface, the chromium (VI) removal efficiency during irradiation process should be decreased.

4.6 Experiment 5 - effect of TiO₂ coating surface area

TiO₂ coating surface of catalyst in this study were varied as 18, 15, 12, 9 and 6 plates. The coating surface area of TiO₂ approximately 104 cm²/plate. The fixed parameters in this research were set at 50 ppm of initial chromium (VI) concentration of 20 L synthetic wastewaters. The flow rate of wastewaters was set at 80 mL/sec as obtained from experiment 3. The water level of wastewaters was set at 4 cm as

obtained from experiment 4. The initial pH for photocatalysis reaction was performed as pH 3 as obtained from experiment 2.

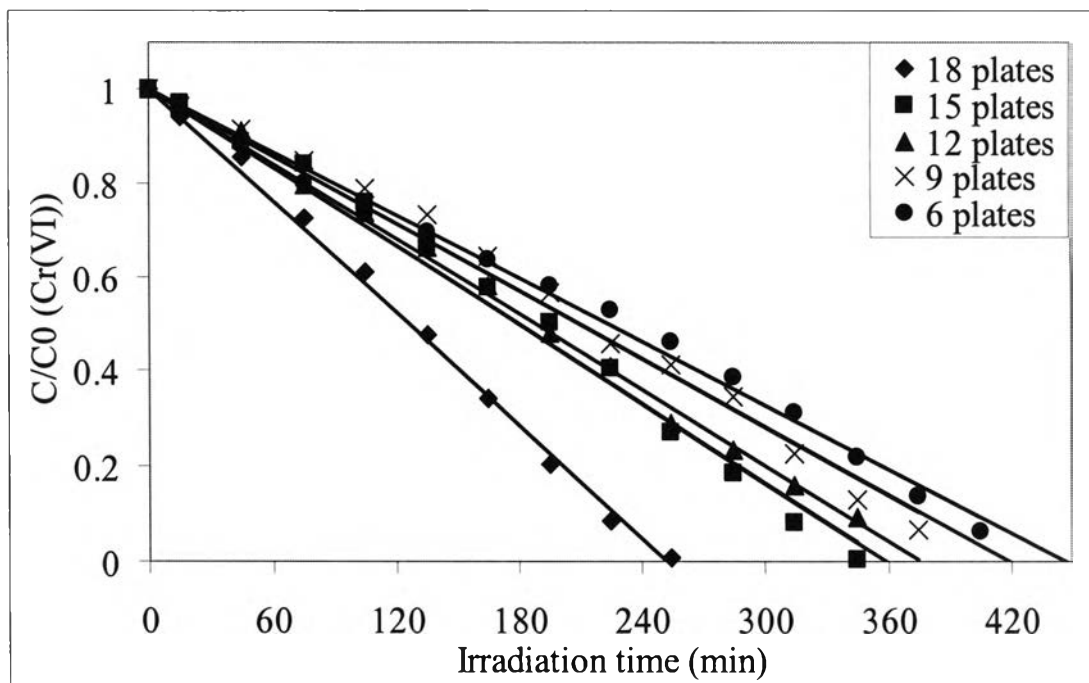


Figure 4.15 Effect of TiO_2 coating surface area on photocatalytic-reduction of chromium (VI) with time ($[\text{Cr}(\text{VI})] = 50 \text{ ppm}$, $\text{pH} = 3$, flow rate 80 mL/sec and water level 4 cm)

From figure 4.15, it was found that when TiO_2 coating surface area increased, the photocatalytic-reduction of chromium (VI) was increased. With full set (18 plates) the fixed bed photoreactor could remove completely 50 ppm of chromium (VI) within 253 minute. As the decreasing of the number of plates, it decreased photocatalytic-reduction of chromium (VI) and spent more time to remove all chromium (VI) in the water. Table 4.5 shows the calculation of important parameters in TiO_2 coating surface experiment.

From Figure 4.15 the kinetic chromium (VI) degradation was zero order. The kinetic coefficient can also be calculated by zero order equation as shown in Equation (7) chapter 2. From Figure 4.16, it was observed that high kinetic coefficients can be obtained at high TiO_2 coating surface area. The highest kinetic coefficients equaled to 0.1978 mg/L.min was observed at full set (18 plates) applied to the system that

contained the highest TiO₂ coating surface area. At the minimum value of the TiO₂ coating surface area (6 plates), the kinetic coefficient equaled to 0.1119 mg/L.min. Figure 4.16 and Table 4.5 it can be summarized that the TiO₂ coating surface area was a function of photocatalytic-reduction efficiency of chromium (VI). Because at high TiO₂ coating surface it contained high amount of TiO₂ which effect on photoactivity.

Table 4.5 Experimental conditions and calculation of important parameters in variation of TiO₂ coating surface area

Parameter	Experiment				
	18	15	12	9	6
Number of plate	18	15	12	9	6
TiO ₂ coating surface, (cm ²)	1,872	1,560	1,248	936	624
Amount of TiO ₂ , (g)	0.3600	0.3000	0.2400	0.1800	0.1200
Cr(VI) removal percentage at 253 min of reaction period, (%)	100	75.9	68.31	60.72	55.66
Kinetic coefficient (<i>k</i>), (mg/L.min)	0.1978	0.1475	0.1327	0.1194	0.1119
Reaction time to complete photoreduction of Cr(VI), (min)	253	338	377	419	447

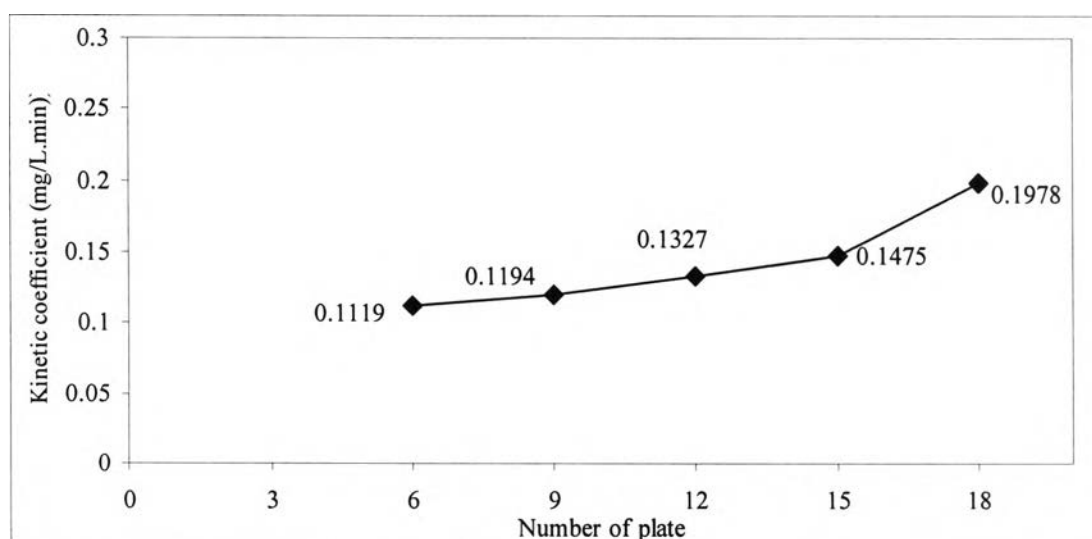


Figure 4.16 Kinetic coefficients (*k*) of chromium (VI) with different TiO₂ coating surface area

From Figure 4.15 and 4.16, it was observed that at 18 plates the kinetic coefficient is drastically increased. This behavior might be due to the result of the higher deposition of TiO_2 on stainless steel plate during the sol-gel process that caused the unusual increasing amount of TiO_2 .

4.7 Experiment 6 - effect of initial concentration of chromium (VI)

To study the effect of water initial concentration of wastewaters on photocatalytic reduction of chromium (VI), the initial concentrations of chromium (VI) in this study were varied as 25, 30, 50, 100, 150, 200, 300 and 500 ppm. The fixed parameters in this research were set at 20 L synthetic wastewaters. The feed flow rate of wastewaters was set at 80 mL/sec as obtained from experiment 3. The water level in the fixed bed reactor was set at 4 cm as obtained from experiment 4. The number of plates was full set (18 plates) as obtained from experiment 5. The initial pH for photocatalysis reaction was performed as pH 3 as obtained from experiment 2.

From Figure 4.17, 4.18 and Table 4.6, it was found that the chromium (VI) degradation in the range of initial concentration of 25-100 ppm was followed zero order pattern. The kinetic coefficient (k) can also be calculated by zero order equation as shown in Equation (7) chapter 2. The chromium (VI) degradation in the range of initial concentration of 150-500 ppm was followed pseudo-first order pattern which can be calculated the pseudo-first order kinetic coefficient (k_{obs}) by pseudo-first order equation as shown in Equation (10) chapter 2. It showed that the kinetic pattern was changed to pseudo first order model at high initial concentration of chromium (>100 mg/L). Table 4.6 showed the comparison of R^2 values, kinetic coefficient and pseudo-first order kinetic coefficient for each initial concentration of chromium (VI) in the range of 25 – 500 ppm.

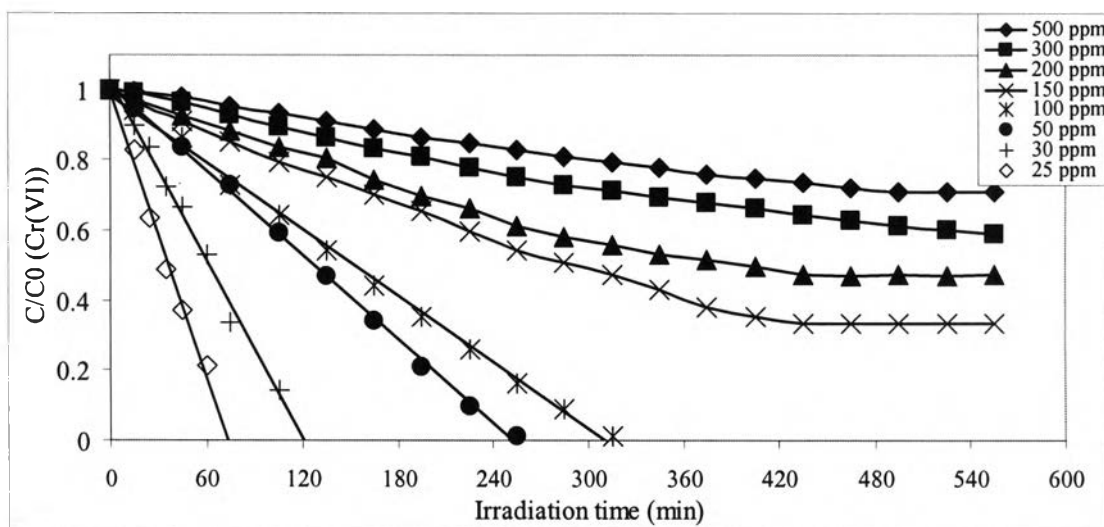


Figure 4.17 Effect of initial concentration of chromium (VI) on photocatalytic reduction of chromium (VI) with time (pH = 3, flow rate 80 mL/sec and water level 4 cm)

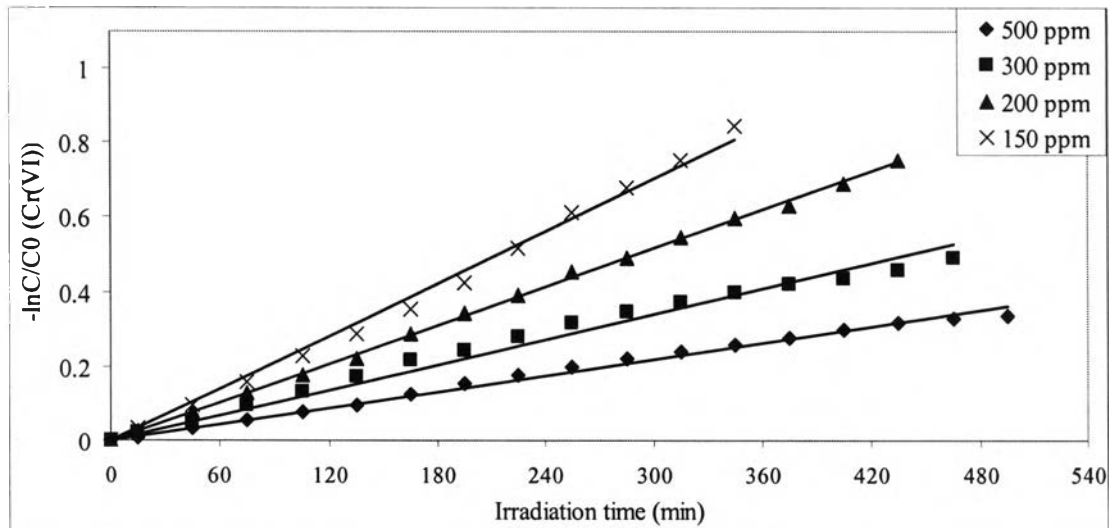


Figure 4.18 Linear transform $-\ln C/C_0$ vs time with different initial concentrations of chromium (VI) in the range of 150–500 ppm

Table 4.6 Determination of reaction order with different initial concentrations of chromium (VI)

Concentration (ppm)	Zero order		Pseudo first order	
	$k, (\text{mg/l.min})$	R^2	$k_{obs}, (\text{min}^{-1})$	R^2
25	0.338	0.9898	0.0228	0.9593
30	0.2501	0.9918	0.0159	0.8445
50	0.1978	0.9984	0.0115	0.6687
100	0.1609	0.9976	0.0077	0.7947
150	0.2491	0.9871	0.0024	0.996
200	0.2572	0.9741	0.0017	0.999
300	0.2636	0.9345	0.0011	0.9782
500	0.3206	0.9807	0.0007	0.9927

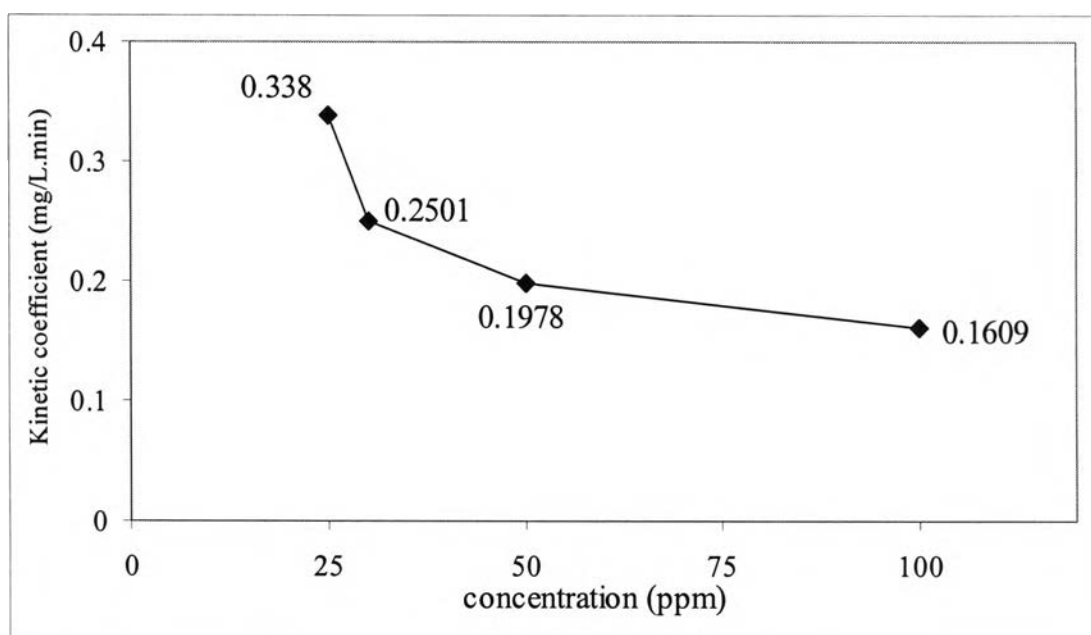


Figure 4.19 Kinetic coefficients (k) with different initial concentration of chromium (VI) in the range of 25 to 100 ppm.

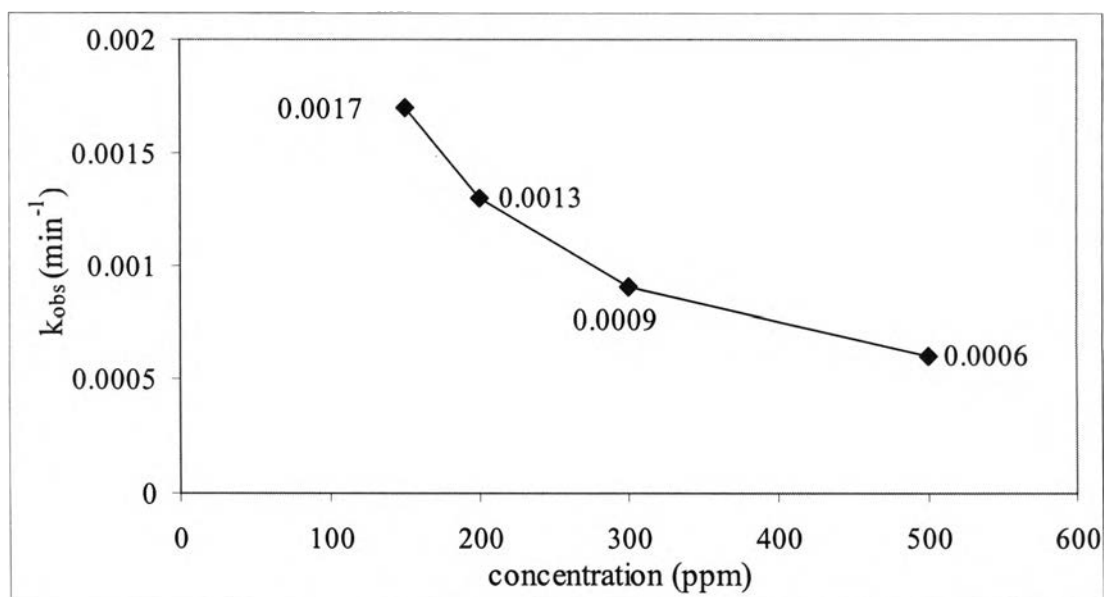


Figure 4.20 k_{obs} with different initial concentration of chromium (VI) in the range of 150 to 500 ppm

Figure 4.19 and 4.20 showed kinetic coefficients and k_{obs} with different initial concentration of chromium (VI). From these figures, the chromium (VI) removal decreased with the increasing of initial concentration. The reason probably might be due to the fact that amount of photo reactive site on TiO_2 surface has been fixed while the initial concentration of chromium (VI) increased. With the limited of TiO_2 surface site to be react with chromium, the chromium (VI) removal can not further react effectively the chromium color is stronger that might absorb a significant amount of UV radiation rather than the catalyst and this might also reduce the catalytic efficiency. Figure 4.21 shows the color of chromate solution with different initial concentration.

From pseudo-first order equation and Figure 4.18, the k_{obs} of each concentration were shown in Table 4.6. Relationship between k_{obs} vs C could be determined in term of the modified empirical Langmuir-Hinshelwood equation. From this equation and Table 4.6, it can be plotted relational graph of $\frac{1}{k_{obs}}$ vs C that shows in Figure 4.22.

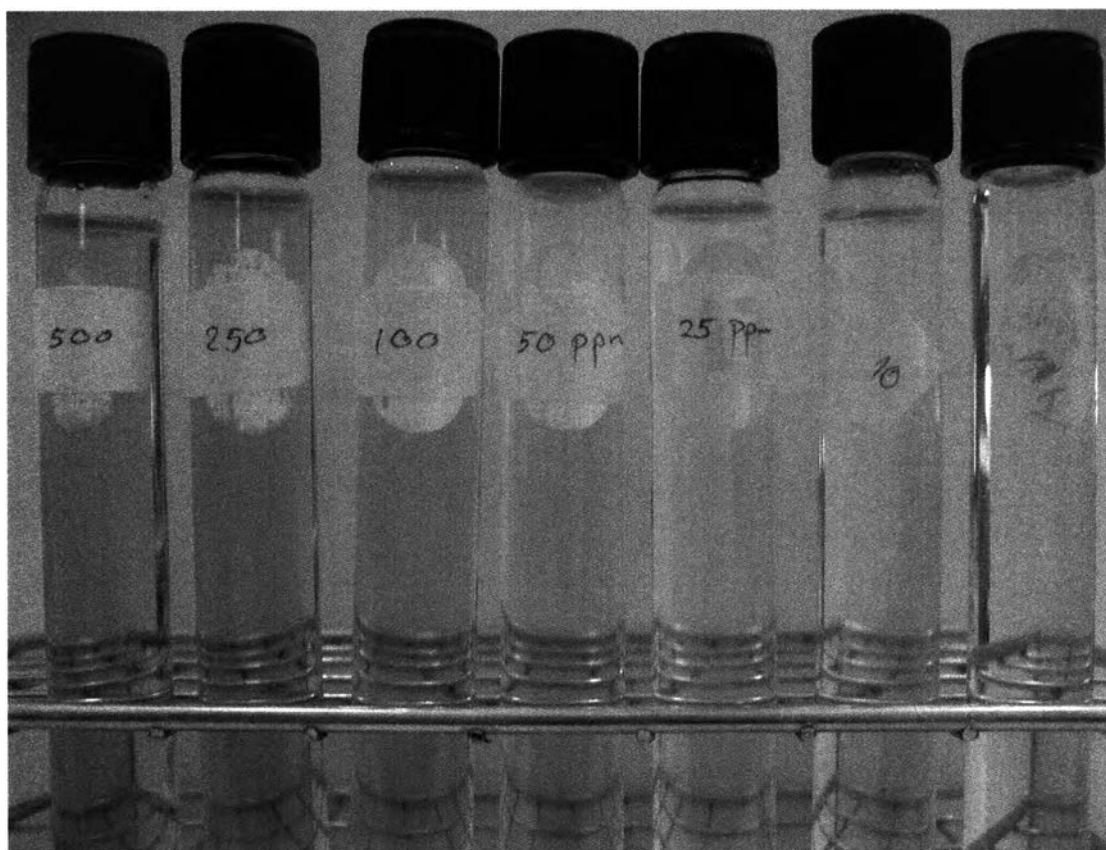


Figure 4.21 Chromate solutions with different initial concentration of chromium (VI)

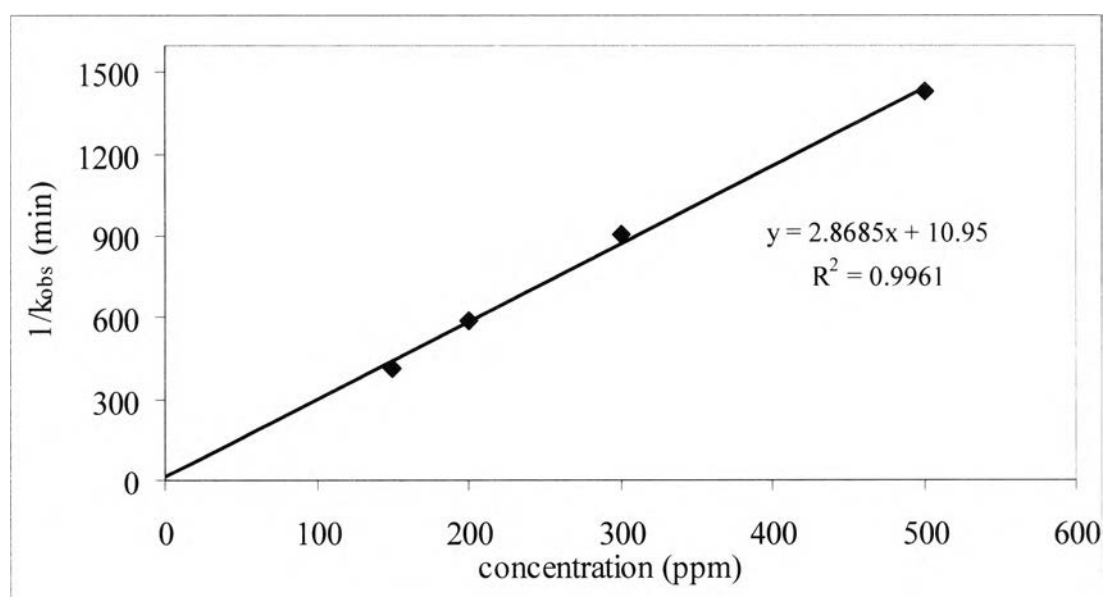


Figure 4.22 Determination of the adsorption equilibrium constants and degradation rate constants

Determination of the adsorption equilibrium constants (K) and degradation rate constants for chromium (VI) (k) could obtained from Figure 4.22. The k was

$$0.3486 \frac{\text{mg}}{\text{l}\cdot\text{min}} \text{ and } K \text{ was } 0.2620 \frac{\text{l}}{\text{mg}}.$$

